DE GRUYTER OPEN

Analele Universităţii de Vest din Timişoara
Vol. LIX, 2016
Seria Fizică

DOI: 10.1515/awutp -2016-0002

LASER HEATING OF THE CORE-SHELL NANOWIRES

Iordana Astefanoaei[1], Ioan Dumitru and Alexandru Stancu

Physics Department, Alexandru Ioan Cuza University, Iasi, Romania

[1] *Corresponding author*: iordana@uaic.ro

Article Info	Abstract
Received: 01.11.2016 *Accepted: 21.12.2016* **Keywords:** Laser, Nanowires, Stress	The induced thermal stress in a heating process is an important parameter to be known and controlled in the magnetization process of core-shell nanowires. This paper analyses the stress produced by a laser heating source placed at one end of a core-shell type structure. The thermal field was computed with the non-Fourier heat transport equation using a finite element method (FEM) implemented in Comsol Multiphysics. The internal stresses are essentially due to thermal gradients and different expansion characteristics of core and shell materials. The stress values were computed using the thermo elastic formalism and are depending on the laser beam parameters (spot size, power etc.) and system characteristics (dimensions, thermal characteristics). Stresses in the GPa range were estimated and consequently we find that the magnetic state of the system can be influenced significantly. A shell material as the glass which is a good thermal insulator induces in the magnetic core, the smaller stresses and consequently the smaller magnetoelastic energy. These results lead to a better understanding of the switching process in the magnetic materials.

1. Introduction

The magnetic nanowires with core-shell structure have received a significant attention due to their special magnetic properties in comparison with bulk materials. In the last years, the core-shell nanostructures as nanowires or nanoparticles are intensively used in the heat assisted magnetic recording (HAMR) [1, 2]. As the name suggests HAMR is a technological procedure in which high anisotropy magnetic systems can be switched with rather small fields because during the switching process the material is temporarily heated [3-6]. As we aim to study a particular magnetic system (core-shell wire) under the heating produced by an electromagnetic field (a LASER beam) we wish to give emphasis to the effect of thermal stresses in the system during the heating process on the magnetization processes. Essentially, this paper is focused on the study of the thermal stresses produced by a laser source placed at one end of a core-shell magnetic nanowire. The external surface of shell is in contact with an external medium which is

maintained at a constant temperature (thermostat). The other end of the wire (opposite to the one heated by the laser spot) could be maintained at the external medium temperature or can be covered with shell material. At the beginning of the heating experiment the entire system is at the medium temperature. Continuity conditions at the core-shell and shell-medium interfaces were imposed for the heat flux.

A numerical 3D spatio-temporal model was developed to evaluate the behavior of thermal field and thermal stresses for the considered system. In the first step, the non-Fourier heat conduction equation was solved in Comsol Multiphysics, using finite element method (FEM), in order to find the temperature distribution. The stresses inside the core are computed by solving the thermo-elastic equations in FEM and using the obtained temperature distribution. The temperature and stress distributions of the core-shell system were analyzed in time as a function of initial temperature of the system, laser power and some geometric parameters (radius, shell thickness and length). The temperature decreases along the axial direction from a maximum temperature corresponding to the laser position to the opposite end of wire. On radial direction the temperature decreases from centre to the external surface. The temperature profile generates a thermal stress distribution in the core-shell system. These thermal stresses are decreasing along Oz direction following the same behavior as thermal gradients. High values of the thermal gradients appear in core-shell systems on axial direction if the end of the system is maintained at the external medium temperature. The thermal gradients decrease considerably if the end of the system is included in shell.

2. The spatio-temporal the temperature and stress during laser heating

2.1 Thermal field analysis

The spatial-temporal temperature distribution is computed in a core-shell nanowire heated by a laser source as a heating source placed at one end of the wire as shown in Figure 1. The wire as a core of the system has the radius R_i, the shell thickness is given by $R_2 - R_1$ where R_2 is the shell radius. The length of this structure is L.

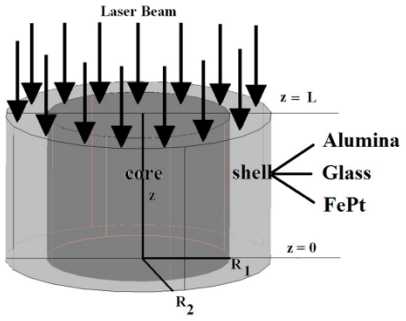

FIGURE. 1 Schematic diagram of the core-shell system

Due to the system symmetry we have used cylindrical coordinates that allows the transformation of the 3D problem in a 2D one (in radial, r, and axial, z, coordinates). The radial coordinate is r = R_1 at core – shell interface and r = R_2 at external surface of the core-shell system. The axial coordinate z is ranged between $z = L$ and $z = 0$, where L is the length of the system. A laser pulse is applied on the upper part of the system at the level $z = L$, for a finite time t_p (Fig.1). The laser light with a considered Gaussian profile on radial direction has the distribution in core:

$$Q_1[r] = Q_{0-1} \exp\left[-\frac{r^2}{R_2^2}\right] \; Q_{0-1} = \frac{P}{\pi R_1^2} \tag{1}$$

and shell:

$$Q_2[r] = Q_{0-2} \exp\left[-\frac{r^2}{R_2^2}\right] \; Q_{0-2} = \frac{Q_{0-1}}{r_1^2 - 1} \tag{2}$$

The parameter r_1 is given by $r_1 = \frac{R_2}{R_1}$. The state of the system is described by the temperature distribution $T_i = T_i\,(r, z, t)$, (i = 1, 2). The index i = 1 denominates the core and the index i = 2 denominates shell. The temperature distribution T_i in the core-shell system was computed as solution of time dependent heat conduction equation (non-Fourier heat transport equation [7]) with proper thermal boundary conditions at core – shell interface:

$$\alpha_i \Delta T_i = \frac{\partial T_i}{\partial t} + \tau_i \frac{\partial^2 T_i}{\partial t^2}; \text{(i = 1,2)} \tag{3}$$

where: $\alpha_i = \frac{k_i}{\rho_i c_i}$ the thermal diffusivity, $\rho_i = \rho_i\,(T)$ is the mass density, $c_i = c_i\,(T)$ is the specific heat capacity and $k_i = k_i\,(T)$ is the thermal conductivity for core and shell. τ_i (i = 1, 2) are the temperature relaxation times [7]. The equation (3) was solved in Comsol Multiphysics

using a finite element method (FEM). In order to consider all the thermal exchanges between core-shell system and the external surrounding medium, another shell named medium shell was added to the system from **FIGURE.1**. In the heating process, the medium shell has the role to receive the all the heat losses coming from the core-shell nanowire system. The medium shell is considered having the same material as system shell, this giving the possibility to extend the model to a big number of core-shell nanowires. The medium shell thickness is R_3 - R_2, where R_3 is the external radius of the medium shell. At the beginning of the laser heating process the core, shell and external medium are in thermal equilibrium at the temperature T_0. The following boundary conditions were imposed on core – shell interface:

- 1) The thermal interaction of the laser radiation with the core-shell systems analyzed in this paper is modeled as a surface heat source, because the absorption length $l_{abs} = \alpha^{-1}$ is less than the heat diffusion length, $l_{th} = 2\sqrt{\frac{k_i\, t}{\rho_i\, c_i}}$, (labs << lth) [6]. α is the absorption coefficient of the material [8, 9, 10]. The thermal flux inside the core and shell is linearly dependent on the temperature gradient along axial direction [11]. In the core, the heat flux is described by

$$-k_1(T)\left.\frac{\partial T_1}{\partial z}\right|_{z=L} = Q_1(r) \tag{4}$$

and

$$-k_2(T)\left.\frac{\partial T_1}{\partial z}\right|_{z=L} = \frac{Q_2(r)}{r_1^2-1} \tag{5}$$

in the shell.

- 2) The lower part of the core-shell system at the level z = 0 and the external surface of the medium shell are kept at the temperature T_0.
- 3) On the core-shell interface on radial direction, the heat flux coming from core is completely received by the shell:

$$k_1\,(T)\left.\frac{\partial T_1}{\partial r}\right|_{r=R_1} = k_2\,(T)\left.\frac{\partial T_2}{\partial r}\right|_{r=R_2} \tag{6}$$

Also, the heat flux from core-shell system is completely received by the medium shell. Therefore, their heat fluxes on interface r = R_1 must be continuous.

- 4) The temperatures of the adjacent regions are equal.
- 5) The temperature on the external surface of the medium shell is constant

$$T_2\ (r = R_2, z, t) = T_0 \text{ and } T_2\ (r, z = 0, t) = T_0 \quad (7)$$

2.2 Laser – induced thermal stress distribution

The thermal gradients and the mechanical constraints due to elastic properties of two different materials in contact are at the origin of thermal stresses in the core-shell system. In the thermo-elastic formulation, the equations at equilibrium for connected bodies known as the compatibility equations are described in reference [11, 12]. The thermal stress distribution in the core-shell system during the heating process was computed with the temperature distribution inside the core and shell given by (3) with the boundary conditions (4) - (7). The thermal stress components in Cartesian coordinates were obtained as solutions of the compatibility equations [11, 12]:

$$(1 + \upsilon_i)\Delta\,\sigma_{xx}^i + \alpha_i\,(T)E_i\left(\frac{1+\upsilon_i}{1-\upsilon_i}\,\Delta T_i + \frac{\partial^2 T_i}{\partial x^2}\right) = 0$$

$$(1 + \upsilon_i)\Delta\,\sigma_{yy}^i + \alpha_i\,(T)E_i\left(\frac{1+\upsilon_i}{1-\upsilon_i}\,\Delta T_i + \frac{\partial^2 T_i}{\partial y^2}\right) = 0$$

$$(1 + \upsilon_i)\Delta\,\sigma_{zz}^i + \alpha_i\,(T)E_i\left(\frac{1+\upsilon_i}{1-\upsilon_i}\,\Delta T_i + \frac{\partial^2 T_i}{\partial z^2}\right) = 0 \text{ (i = 1, 2)} \quad (8)$$

where x, y and z are the Cartesian coordinates, Δ is laplacean operator, $\alpha_1(T)$ and $\alpha_2(T)$ are the temperature dependence of the thermal expansion coefficients of core and shell materials in contact υ_1 and υ_2 are the Poisson`s coefficients for core and shells. The cylindrical stress components in core and shell were obtained by a coordinate transformation [11, 12] of the Cartesian stress components given by the equations (8). The following conditions were imposed on the core –shell shell interface:

- 1) the mechanical equilibrium condition of stresses at the core-shell interface:

$$\sigma_{rr}^{core}\ (r = R_1, t) = \sigma_{rr}^{shell}\ (r = R_1, t) \quad (9)$$

- 2) the mechanical equilibrium condition of stresses on the external medium surface (r = R_2) of the shell:

$$\sigma_{rr}^{shell}\,(r = R_2, t) = \sigma_{rr}^{m-shell}\,(r = R_2, t) \quad (10)$$

Using the boundary conditions (9) and (10), the components of the thermal stresses in cylindrical coordinates are computed. In the numerical evaluations it was considered that the medium shell is not heated by the laser source. Its role in computation is to evaluate the thermal exchanges through external surface of the core-shell system. In this approach, it was considered that medium shell has not influence on the elastic behavior of the core-shell system.

3. Results and Discussion.

In simulations we considered a FePt core having the radius R_1 = 6.2 nm surrounded by an alumina shell with thickness R_2 - R_1 = 2.8 nm. The total length of the wire was L = 10nm. The system is similar with the ones presented in a HAMR experiment [9]. The spatio-temporal temperature and stress distributions were analyzed considering that the heating process of the system starts from a number of initial temperatures: T_0 = 20K, 100K, 200K 300K. The temperature dependence of thermal characteristics (thermal conductivity and specific heat capacity) and elastic constants was also taken into account.

1) **FIGURE.** 2(a) shows the spatial temperature at time t = 1 ns from the beginning of the heating process. Fig. 2(b) shows the spatial distribution of the radial stresses at the same time moment. As a general characteristic, the temperature and thermal stresses decrease along the radial direction from the centre of the core to the external surface due to Gaussian shape of the laser source. Also, as it was expected, the values of temperature and thermal stresses respectively, decrease along z direction from the level z = L to the level z = 0.

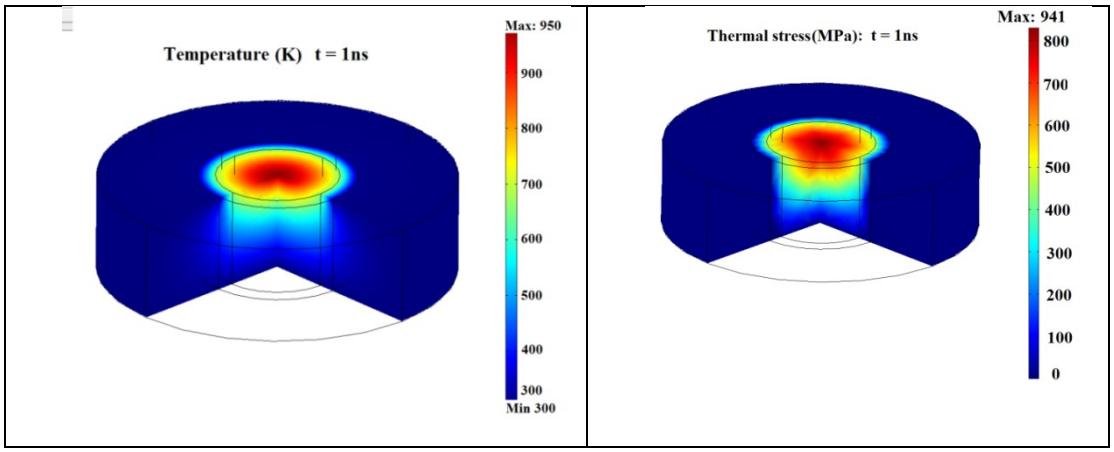

(a) (b)

FIGURE. 2 (a) The spatial temperature distribution in the core-shell system at t = 1ns; (b) The radial stress distribution in the system at t = 1ns;

2) **FIGURE.** 3 (a) shows the time evolution of temperature at the point (r = 0, z = 9 nm), considering that the heating process of the system starts from the following initial temperatures: T_0 = 20K, 100K, 200K, 300K. The laser power was maintained at P = 1.5 mW in all simulations. As a general characteristic, the temperature increases until the thermal equilibrium of core-shell system is attained.

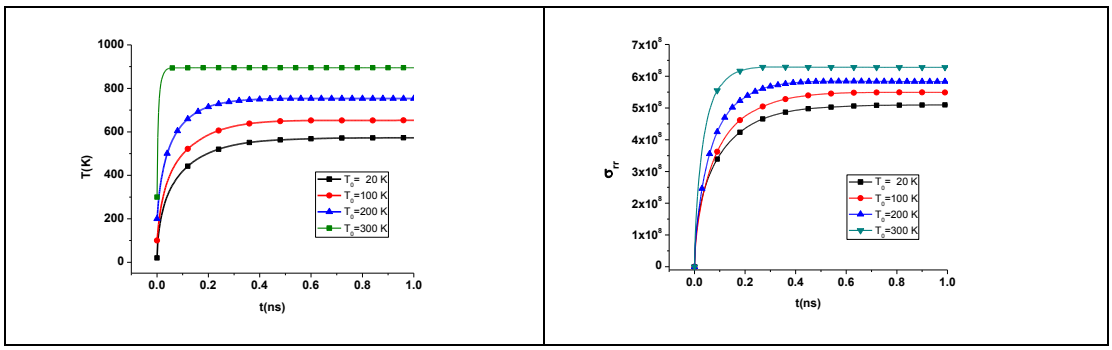

(a) (b)

FIGURE. 3 (a) The time evolution of temperature at the point (r = 0, z = 9 nm) in core for different initial temperatures of the system. (b) The time evolution of thermal stresses.

For example, the core-shell system reaches the thermal equilibrium in about one nanosecond if the initial temperature of the system is T_0 = 20K. The thermal equilibrium of the system is reached in a longer time if the system is heated starting from a smaller temperature. Also, the

temperature at the thermal equilibrium is smaller when the initial temperature of the system is smaller. The time evolution of the thermal stresses in the same point (r = 0, z = 9 nm) is represented on the **FIGURE 3**(b). One observes that the temperature profile influences the thermal stress behavior. The thermal stresses also depend on the initial temperature of the system. At thermal equilibrium the system reaches the mechanical equilibrium. Therefore, if the initial temperature of the system is T_0 = 20K the system needs around one nanosecond to reach the mechanical equilibrium.

3) **FIGURE. 4** describes the temperature and stress field at the thermal equilibrium, at the center of the FePt core, on axial direction ((a) and (b)) and radial direction ((c) and (d)). The heating process of the system starts from temperature T_0 =300 K. In the simulations the shell materials with different thermal characteristic were chosen. The shell was considered from same material as the core and then from materials with lower conductivity: glass and higher conductivity: alumina. The wire is covered with shell excepting the top side where the laser spot is applied. This figure shows the temperature along axial direction, the positive value represent the region inside the wire (0 – 10 nm), the negative direction correspond to shell region (-10 nm - 0). The external surface of the shell is kept at the room temperature. The temperature and stress distribution were considered after a time long enough to obtain the thermal equilibrium. If the shell is alumina, the material with intermediate thermal conductivity, the temperature increases in axial direction from the room temperature to a maximum temperature at the heated end. A small slope discontinuity is observed at the core - shell interface. The glass shell ensures a higher temperature in the wire due to the good thermal insulation properties. The temperature slope decreases in the core, on axial direction, compared with the slope obtained for alumina shell, but increases in the shell. In the case of FePt shell the temperature inside the wire is below that the obtained for alumina shell due to the higher thermal conduction of FePt that provide a better transmission of the heat to the external medium. A higher thermal gradient direction induces a stronger variation of thermal stresses on z direction. The thermal gradient on z direction is given by the slope of the curve which represents the temperature values on z direction. The value of the slope depends on the thermal and elastic conditions which are imposed at the end of the system (z = 0). If the wire end is kept at the value of external medium T_0, in mechanical equilibrium, the value of the slope is higher for both temperature and stress axial dependence.

Considering that the cold end of the system (z = 0) is included into the shell and considering two materials (alumina and glass) for shell we have also simulated the temperature and stress distribution. The slopes of the temperature and stress curves become smaller. The use of a shell at the end of the system allows a decrease of the thermal flux cumulated in system. The thermal gradients along axial direction are smaller if the end of the system is included into a glass shell. The glass materials decreases the thermal stresses on the axial direction. If the end of the system included in alumina shell, a heat amount from the core-shell system is dissipated into added shell due to thermal exchanges between systems. The thermal stress, originated in the thermal gradients of the system, present an important variation along radial and axial directions. The value of the stress, in the GPa range, leads to a magnetoelastic energy in the same order of magnitude as magneto-crystalline energy of FePt core [13]. The smallest values of the stress are obtained in the case of glass shell which is best thermal insulator material analyzed. The highest value is obtained for alumina shell, which has an intermediate value of the thermal conductivity, that is smaller than FePt one. The elastic properties of the core and shell materials in contact, explains his contradictory result.

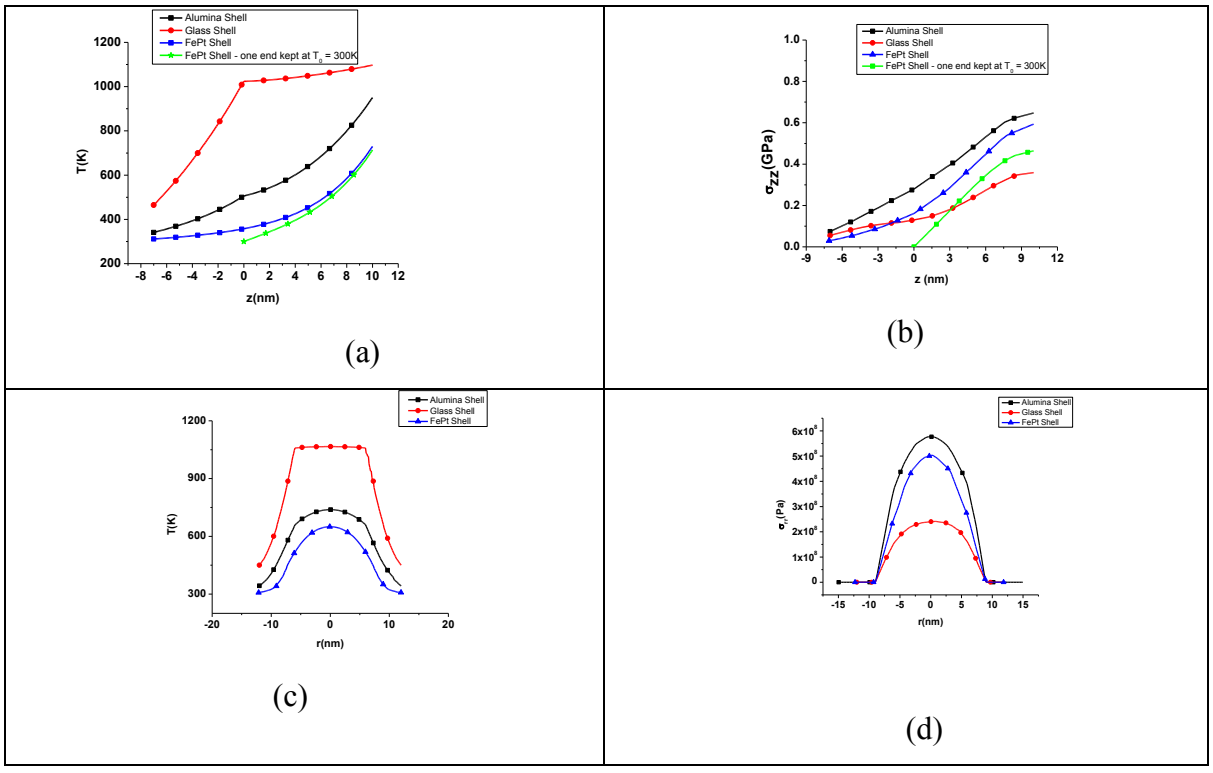

FIGURE. 4 (a) Temperature on axial direction in core for different shell materials. (b) The thermal stresses on axial direction for different shell materials. (c) The temperature on radial direction in core for different shell materials. (d) The thermal stresses on radial direction.

4. Conclusions

The paper presents a phenomenological analysis of the thermal stress distribution produced by a laser as heating source on a core-shell nanowire. The high order of the thermal stress magnitude (GPa) due to the heating leads to a magnetoelastic energy of $8 \cdot 10^5$(J/m3) which is comparable with the magnetocristalline energy of FePt core (approximately $2 \cdot 10^6$(J/m3). As a consequence, magnetic state of the system can be influenced significantly. The high order of the thermal stress magnitude (GPa) due to the heating leads to a magnetoelastic energy with the same order of magnitude as magneto-crystalline energy of FePt core. Therefore, the magnetoelastic energy of the core could influence the magnetic state of the core. Different shell materials lead to different thermal stresses values in the magnetic core. A glass shell ensures a better thermal insulation and lower thermal gradients than alumina shell. The thermal stresses are lower for glass shell, than alumina shell. The control of the thermal stress in the core-shell system is obtained for different shell materials and size parameters of the system (radius, length, shell thickness). The thermal stress at the end of the laser heating process becomes an important parameter which needs to be carefully analyzed in the heating treatments of the magnetic materials.

Acknowledgement

Work was supported by Romanian CNCS-UEFISCDI Grant Nos. PN-II-RU-TE-2012-3-0449.

References

[1] S. Sun, C. B. Murray, D. Weller, L. Folks, A. Moser, Science, **287**, 1989–1992 (2000).

[2] Sh. Kang, Z. Jia, D. E. Nikles, J. W. Harrell, IEEE Transaction on Magnetics **39,** 5 (2003).

[3] B. X. Xu, Z. J. Liu, R. Ji, Y. T. Toh, J. F. Hu, J. M. Li, J. Zhang, K. D. Ye, C. W. Chia, Journal of Applied Physics, **111**, 07B701 (2012).

[4] S. Saranu, S. Selve, U. Kaiser, L. Han, U. Wiedwald, P. Ziemann, U. Herr, J. Nanotechnol., **2** 268-275 (2011).

[5] W. Wang Hai Dong et all, Chinese Science Bulletin **57**, 24 (2012).

[6] J. Buschbeck et all, J. Appl. Phys. **100**, 123901 (2006).

[7] COMSOL Multiphysics, Heat Transfer Module and Structural Module.

[8] A. Helebrant, C. Buerhop, R. Weiβmann Glass Technology **34** 4 (1993).

[9] C. J. Smitthels, Metals Reference Book.

[10] F. Cardarelli, The Handbook of Optical Materials.

[11] B. A. Bosley, J. H. Weiner, Theory of Thermal Stresses, Wiley, New York (1960).

[12] N. Noda, R. B. Hetnarski and Y. Tanigawa, Thermal Stresses, 2nd ed. Taylor and Francis, New York (2003).

[13] S. N. Hsiao, S. H. Liu, Applied Physics Letters **101**, 182404 (2012).